A Comparative Analysis of Nanoparticle Type Variants for Plasmonic Light Trapping Enhancement in Thin Film Hydrogenated Amorphous Silicon Solar Cells

Chetan Radder*, B S Satyanarayana**

* Electronics Engineering, Jain University, Bangalore, India

** BML Munjal University, Sidhrawali, Gurgaon, India

(chetanradder89@gmail.com, satyang10@gmail.com)

‡ Chetan Radder, Electronics Engineering, Jain University, Bangalore,

Tel: +91 9481107705, chetanradder89@gmail.com

Received: 12.04.2018 Accepted:08.06.2018

Abstract-. The new possibilities for the photoelectric conversion enhancement of solar cells are explored by the phenomenon of plasmonics with nanoparticles (NPs) having higher charge carrier concentration deposited on to the substrate with the intention of meeting the energy demands by renewable sources over the fossil fuels. A systematic simulative analysis is performed to understand the role of different material types of NPs on the thin film hydrogenated amorphous silicon (a-Si:H) solar cells upon deposited on the front surface exposed to the incident light radiations. The three-dimensional simulations with finite difference time domain approach are performed to monitor enhanced optical absorption induced by localized surface plasmon, quantified by the near-field concentration and the modelled scattering and absorption cross-sections of nanoparticles in the interesting range of wavelength. The paper investigates the plasmonic coupling of light into thin film a-Si:H structures in terms of dielectric properties providing an option to narrow down to cost-effective nanoparticles for the enhanced performance across the visible range of the spectrum in the interest of large-scale manufacturability. The search for new functional NP materials covering noble metals and few nitrides and their contribution to light trapping enhancement is analysed for obtaining the highest device absorption with low NP parasitic absorption. The modelled plasmonic structures generate higher device scattering with aluminium and beryllium NPs in the ultra-violet (UV) region, followed up by silver, copper, chromium, nickel, platinum, titanium, tungsten in the visible region and near to infra-red (IR) region it is with gold and palladium NPs at their corresponding resonance wavelengths. The observed resemblances of resonances of low-cost nitrides TaN, ZrN with gold and HfN with silver helps us to shift towards cost-effective thin film plasmonic solar cells. For the optimal design of thin film a-Si:H solar cell, it's demonstrated by the obtained results that the NP type is a choice between the dominant scattering over the undesired reflection and parasitic losses.

Keywords Plasmonics; Metal nanoparticles; Thin film solar cells; Light trapping; Hydrogenated amorphous silicon solar cells; Photovoltaics;

1. Introduction

The thin film materials with the reduced material and fabrication costs can replace conventional thick film materials in solar structures and with improved conditions for carrier collection can result in higher conversion efficiencies [1]. The ability to support over a wide range of cost-effective substrates covering rigid (glass, building facades and rooftops [2]) and flexible (plastics [3]) makes thin film materials an ideal choice for the ever-expanding PV requirements and to multiple consumer-oriented applications[4]. The high nature abundant and lightweight hydrogenated amorphous silicon (a-Si:H) with properties like low toxicity and flexibility makes it an attractive option for

solar cell applications[5]. In thin film a-Si:H structures, the optical path length is drastically reduced due to thin absorbing electrical layers with poor light absorption in red and near-infrared regions. The metallic nanostructures deposited on the front surface of a thin film solar cell offers a potential way for higher light trapping in the visible range of spectrum [6] with reduced initial reflection at the surface.

The electromagnetic interaction of the incident light radiations with plasmonic nanoparticles (NPs) excites the cloud of free electrons across the surface getting into localized surface plasmon (LSP).An Electromagnetic excitation of transverse-magnetic (TM) kind with an electric field perpendicular to surface propagates a wave-like fashion along the interface between metal and the thin film dielectric medium, termed as Surface plasmon polariton (SPP) [7] resulting in light being trapped surrounding NPs as the LSP mode. At a particular resonating frequency, plasmonic NPs will have a very strong interaction with the incident light as the optical cross section exceeds geometrical cross section[8] inducing a localized surface plasmon resonance (LSPR). With the excitation of LSPR, incident light is confined in the vicinity of NPs by the local electromagnetic field enhancement resulting in enhanced light absorption covering low light capacity for thin film solar cells. The excitation of LSPs by NPs of the size smaller than the wavelength of the light give rise to scattering and/or absorption of the incident light. The mechanism of scattering and absorption are metal type, size and shape dependent [9] and are to be fine-tuned to alter the contribution of each mechanism for higher device light absorption.

In the light interaction with NPs, an effect of scattering is associated with undesired parasitic absorption resulting in heat being generated, leading to a loss mechanism where radiations are blocked by entering into the active photovoltaic layers. Contrary to that, the NPs with the resonant absorption at wavelengths out of a-Si:H absorption range will drastically reduce the undesired parasitic absorption. In a highly light trapping structure, incident electromagnetic waves are concentrated into the thin film by multiple and high-angle scattering increasing the effective optical path length before escaping out of the device [10]. A great deal of research in thin film solar cells is focused on light management schemes for light trapping optimization with the enhanced absorption in the active layer by total utilization of above bandgap photons. This paper explores light trapping enhancement in thin-film a-Si:H solar cells with respect to geometric and dielectric sensitive NPs in terms of localised electric field distribution and corresponding scattering/absorption. The NPs with plasmon resonance in and out of the visible region on the front surface of the structures are simulated for complete investigation with an intention of obtaining higher device light absorption.

2. Design and Materials

The thin film a-Si:H solar stack is grown on Indium Tin Oxide (ITO) coated glass where ITO functions as a transparent conducting oxide (TCO) for incident light concentration into the device. The schematic cross section of the single junction a-Si:H considered for simulations is as shown in Fig.1 constituting of 10nm heavily doped p-type, 460nm undoped and 30nm heavily doped n-type. For the plasmonic analysis, the most favourable way of embedding the nanoparticles at the interface of front TCO layer and P-layer of a-Si:H structures is considered as it can reduce initial reflection by diverting the incident rays into the device making it optically thick for electromagnetic radiations [11]. In this work, a Gaussian light spectrum with a wavelength range of 200 to 1100 nm was normally incident on the structure consisting of spherical NPs placed in a square arrangement in the x-z plane and stacked active p-i-n layers stretched across the x-y plane as shown in Fig.1. For the simulations, an idealistic perfectly matched layers (PML) boundary conditions are used across all the three planes. The excitation source for a TM polarized Gaussian wave propagating along the y-direction is placed 200nm above the NPs. The finite difference time domain (FDTD) approach solves Maxwell equations on a discrete grid to calculate electromagnetic field (E, H) within the region of interest. The three-dimensional simulations are carried out using a freely available FDTD package called MEEP [12] covering wide frequency range in a single simulation run.

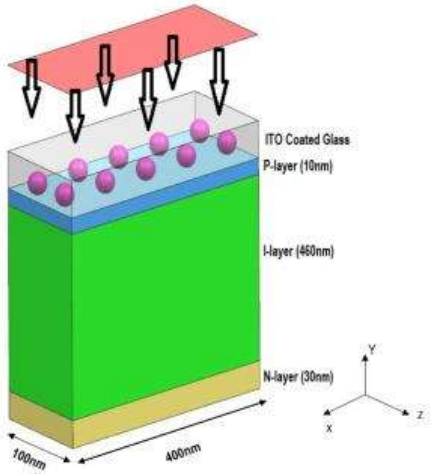

Fig. 1. Cross section of a-Si:H solar cell.

In order to perform realistic simulations, active semiconducting layers and NPs are defined by experimentally obtained optical values. Optical properties of the materials in the simulation region are set by a complex dielectric constant ε'+iε" as a function of wavelength, ε' and ε" stands for real and imaginary dielectric values respectively. The real part of the dielectric value describes how strongly a material can be polarized by an external electric field and the imaginary part describes the losses in the material due to the polarization and ohmic losses [13].The refractive indices of intrinsic, p and n doped a-Si:H are obtained from ellipsometry measurements [14] and the dielectric constant of all wavelength-dependent considered NP materials and ITO are obtained from Ref[16]. The dispersive material properties are explored by converting the wavelength dependent values to Lorentz Drude (LD) model values and are used as material defining parameters in the MEEP compatible scheme code for the simulations.The Drude-Lorentz equation [15] can be written as

$$\varepsilon(w) = 1 - \frac{\sigma_0 \omega_p^2}{\omega(\omega - \mathrm{i}y_0)} + \sum_{j=1}^{k} \frac{\sigma_j \omega_p^2}{(\omega_j^2 - \omega^2) + \mathrm{i}\omega y_j} - (1)$$

where $\varepsilon(\omega)$ is the dielectric function; ω_p is the plasma frequency with oscillator strength σ_0 and damping frequency γ_0; k is the number of oscillators with resonant frequency ω_j, strength σ_j, and damping frequency γ_j. The experimentally obtained real and imaginary dielectric values are converted into the above parameter values by a developed Matlab code and when used for simulations, it defines the realistic properties of materials.

The metal NPs with an abundance of free electrons poses a negative real part and small imaginary part giving rise to resonant scattering due to a sign change in permittivity at a metal/dielectric interface resulting in the circumstance of plasmonics. The NPs with dimensions near to the wavelength of incident radiations in the range of few nanometers are to be modelled to explore the optical properties at the nanometer range. Modelling based on Mie theory is capable of simulating the optical properties of structures in terms of scattering, absorption and extinction cross-sections and the associated efficiencies. For a higher structural efficiency, scattering cross section should be as high as possible with NP absorption cross section as low as possible. Meanwhile, NPs should be capable of scattering most of the radiation into the cell with higher angular spread to maximize the optical path length in the semiconducting layers of the structure. With the incorporation of NPs, losses such as absorption by the NPs (dissipated by heat), charges recombination, shunt currents are observed which are accumulated in simulations considering around 5% margin for efficiencies. In this paper, the optical properties of the metal thin film are investigated focusing on the SPP modes around 500-600nm i.e @ ~1.85 eV, very close to the a-Si:H bandgap which is the most relevant range of wavelengths for light trapping in a-Si:H solar cells. The influence of the NP materials and geometrical parameters on the absorption enhancement for the thin film solar cells has been investigated to obtain the optimized pattern for the high-efficiency solar cells.

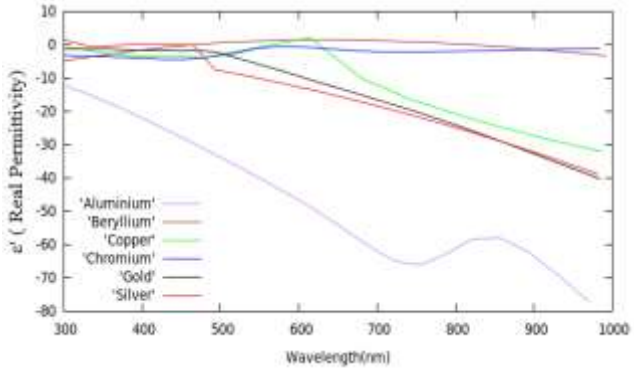

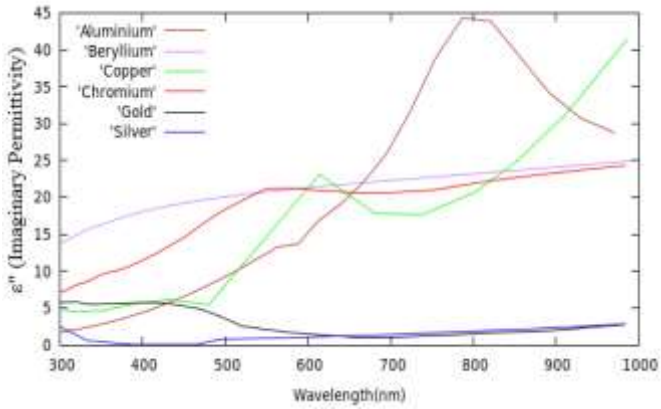

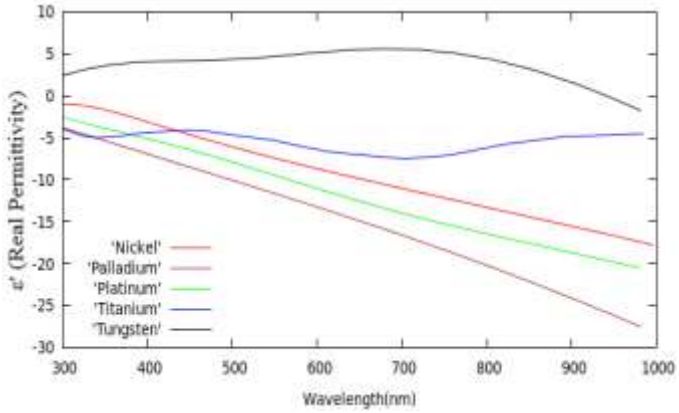

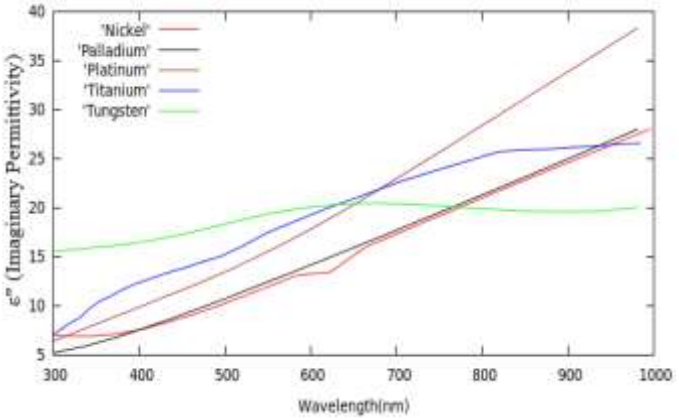

3. Results and Discussion

A comparative study is performed for the considered metal and metal nitrides as NPs in the considered model in terms of enhanced photocurrent due to forward scattering into the device or suppressed photocurrent due to the reverse scattering. In a high permittivity value dielectric, incident light gets concentrated and with closer the NPs to dielectric, relative scattering enhancement is observed.

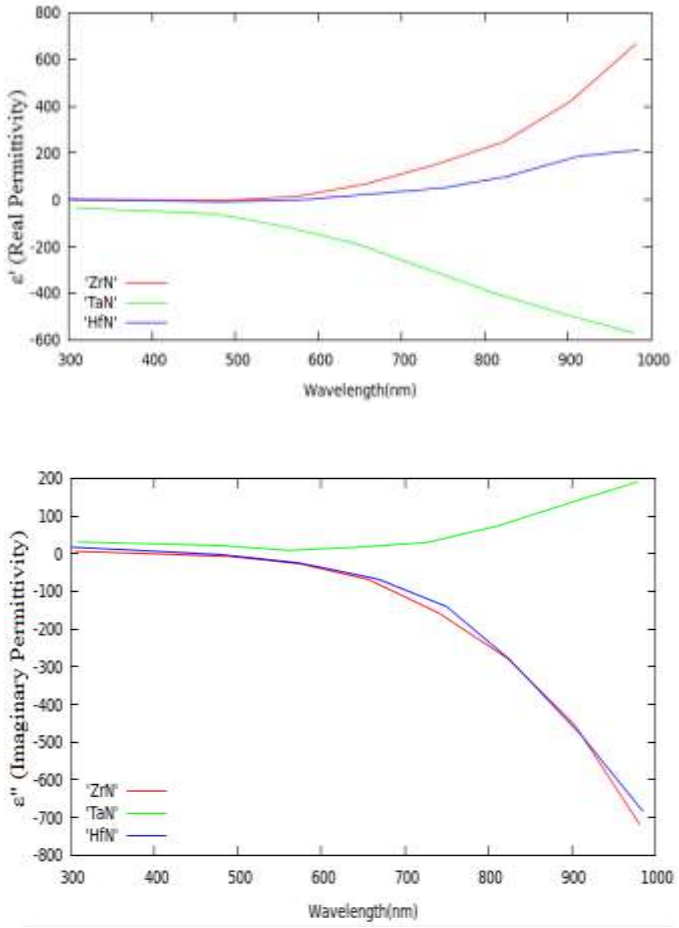

Fig. 2. Real & imaginary permittivity values of NPs for varying incident wavelength.

The enhancement in photo absorption is directly proportional to the increased forward scattering cross section and the higher localised near-field surrounding the NPs within the thickness range of active thin film layers. The generated angular spread of light by the reflection of the light back towards the surface due to NPs enhances the optical light path within the device with the NP parasitic absorption reducing the photocurrent generation. The carried out exercise helps in optimizing the type of metal NPs for silicon solar cell applications to expand upon the wide range of device absorption in terms of device scattering enhancement. The considered metals are defined by its permittivity values obtained from [16] and [17], the graphical representations of value variations with respect to incident wavelength are as shown in Fig.2. In Gold(Au) and Silver(Ag), the ε' values go negative approximately around 327nm and 207nm respectively, the ε' and ε" values have minor variations till 600nm and later follow each other with lower ε" values. In case of copper (Cu), ε' tends to follow the path of gold with relatively less negative values and ε" values are linearly increasing above 500nm. Aluminium (Al) displays a negative ε' at wavelengths less than 200nm with a more negative ε' and higher positive ε" values spread across the visible range compared to Au and Ag at the higher wavelength. A common pattern of ε' and ε" variation is observed in Nickel (Ni), Palladium (Pd) and Platinum (Pt), ε' value becomes more negative with the wavelength shift from violet to red with positive ε" values in the order of Ni, Pt and Pd. In case of Beryllium (Br) and Chromium (Cr), values of ε' and ε" are almost similar with minor variation observed below 550nm with ε' values swinging between positive and negative values near to zero and almost constant ε" without much higher positive values over the spectrum spread. Not many variations are observed in the ε' values of Titanium (Ti) and Tungsten (W) possessing lower negative and lower positive values respectively, ε" is linearly increased in Ti and in W it's constant with the lower value. In the considered nitrides, the typical variation is observed with near to zero values of ε' and ε" till 500nm and at higher wavelengths pattern shift is observed. Above 500nm for TaN, ε' values gradually become more negative and ε" values become more positive and in case of ZrN and HfN, it's the reverse with ε' moving towards positive and ε" towards more negative values.

The carried out work provides a systematic study on scattering and absorption by NPs, exploring several combinations of material and geometrical parameters in order to identify the combinations that could enhance solar cell efficiency. The scope of work covers the role of material permittivity on the device photocurrent enhancement by considering various metals and nitrides as NPs to trap red light into the absorber layer in addition to the already absorbed blue light. For light trapping, it is important that scattering is more efficient than absorption which is seen with comparatively larger nanoparticles [11], in our analysis NPs of dimensions 50nm with a spacing of 75nm are considered. The broader resonance with the suppressed parasitic absorption in NPs is essential for the conversion efficiency enhancement. With the finite real part of the permittivity, incident waves can penetrate through the NPs and field gets attenuated as it cannot be radiated into the thin film a-Si:H layers dissipating the energy as heat. The basic requirement for an efficient plasmonic design is it should have efficient light radiation and low heat loss in metal structures.Noble metals and the corresponding nitrides as NPs with negative value and a-Si:H with the positive value of real part of the dielectric permittivity, supports plasmonic propagation and resonance due to sign change at the interface[7]. The near-field images would allow us to properly link the optical and electrical enhancements with the enhancement in the interaction of electromagnetic fields with the PV cell due to the presence of NPs.

3.1. Structures with Au, Ag, Al and Cu NPs

3.1.1. Ag (Silver)

The photon absorption in the UV-blue-green range is reduced in structures having Ag as front side plasmonic NPs and with the increase in wavelength, device absorption increases till it reaches 690nm. With the corresponding transition outside the visible region of the spectrum, Ag possesses low absorption loss with high radiation making it an ideal choice for solar cell applications. The analysis covers a wide wavelength range from 200nm to 700nm and with the illumination, the rise in resonant peak is observed between 400nm and 500nm. Fig. 3(a) shows the nearby

localised electric field distribution on a front surface of the structure with Ag NPs under the resonance wavelength of 474nm illumination. The corresponding variations of the electric field, scattering and absorption efficiencies with incident wavelength are as shown in Fig. 3(e), Fig. 3(f) and Fig. 3(g). The low imaginary permittivity value of Ag allows plasmon resonance to give rise to highly intense evanescent near-field, localized in a nanoscopic vicinity of the particles surface with far-field propagation [18]. Based on the Mie scattering analysis as per the plot in Fig. 3(f), higher scattering efficiency is observed with Ag NPs compared to other noble metals in the wavelength range of 400-600nm. It is observed that Ag NPs can sustain SPP waves at optical frequencies with very few losses [19].

3.1.2. Au (Gold)

The highly stable Au with reluctance to oxidation, guaranteeing the long life of the device possesses plasma frequency in the visible region. Due to its interband transitions, the observed plasmon resonance is at around 650nm with lower near-field enhancements observed resulting in reduced device absorption with Au as shown in Fig. 3(b). With the noble metals as NPs, near to the surface plasmon resonance the conduction band electrons coherently oscillate to obtain the strongest possible scattering of incident radiations. Au NPs, when placed on the front side of the thin film solar cell, will scatter more light in the forward direction compared to Ag NP as shown in Fig. 3(f) near its resonance. Its seen with Au NPs that scattering to absorption ratio is very low, even with the higher channelling of incident light it is still not an optimal choice owing to higher losses associated with parasitic NP absorption. With the larger Au NPs at and above resonant wavelength, forward scattering within the device is higher with improved scattering to absorption ratio making it a viable option. The computational electromagnetic simulations confirm enhanced device transmission and concentration of generated electromagnetic fields within the absorbing a-Si:H layers and with higher particle density, substantial enhancement can be observed making it a largely used NP for present plasmonic thin-film a-Si:H solar cells.

3.1.3. Al (Aluminium)

In the recent times for plasmonic illustration, the default choice of NP is either Ag or Au covering visible and near-infrared part of electromagnetic spectrum. To overcome the inherent limitations of Ag and Au not exhibiting the plasmonic resonance at blue and ultraviolet (UV) parts, Al is preferred with an intention of covering complete part of the spectrum. The near-field image for a-Si:H substrate with Al NPs is as shown in Fig.3(c) with incident illumination at a wavelength of 303nm within the UV region where Al NPs in its vicinity undergoes strong interaction with the incident radiation. The blue-shifted plasmonic resonance and a suppressed parasitic metallic absorption generated a broader spectral region showing enhanced performance.

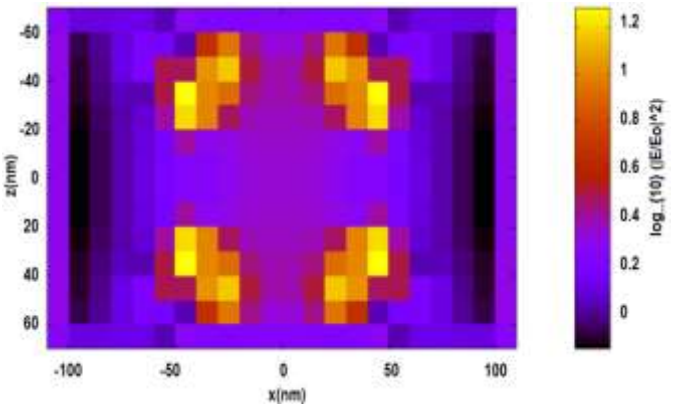

(a) Silver @474nm

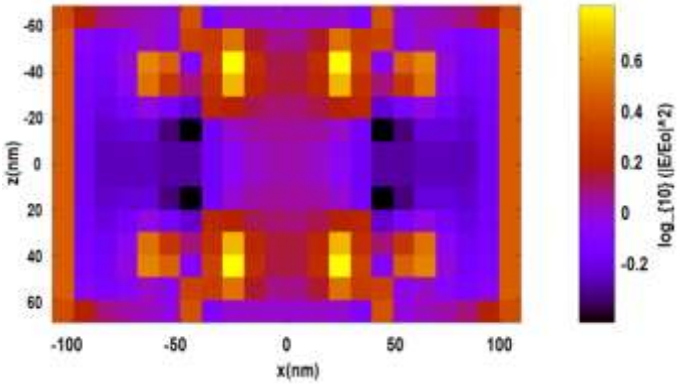

(b) Gold @650nm

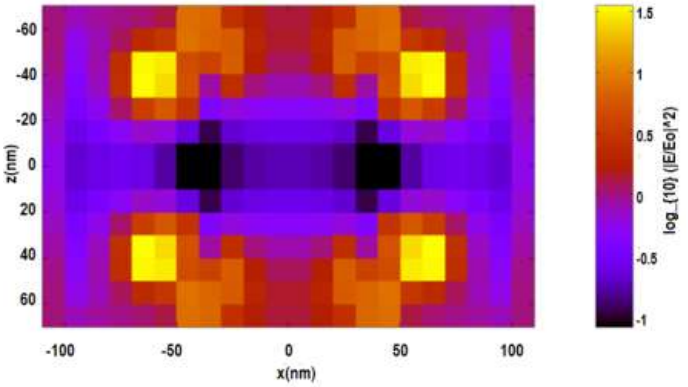

(c) Aluminium @303nm

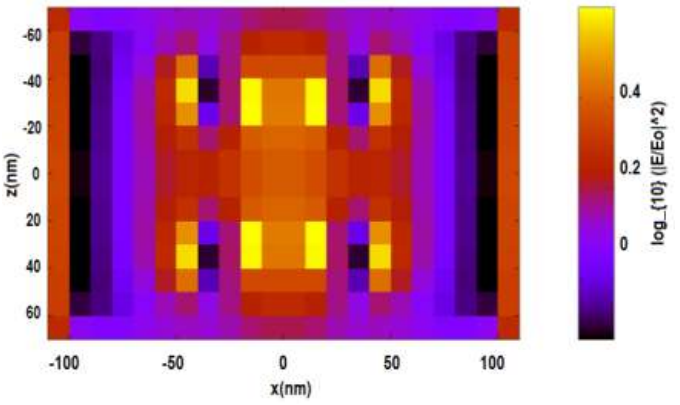

(d) Copper @465nm

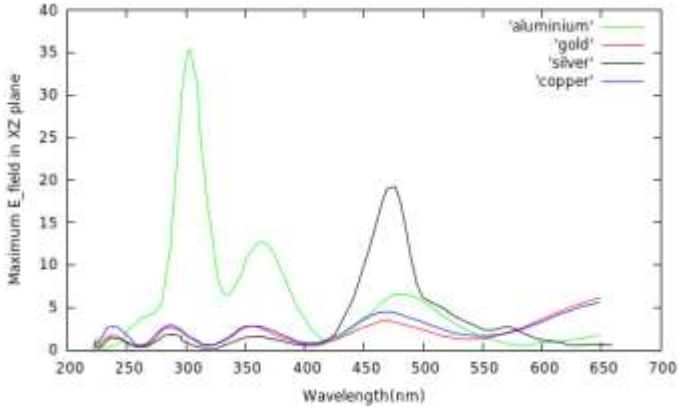

(e)

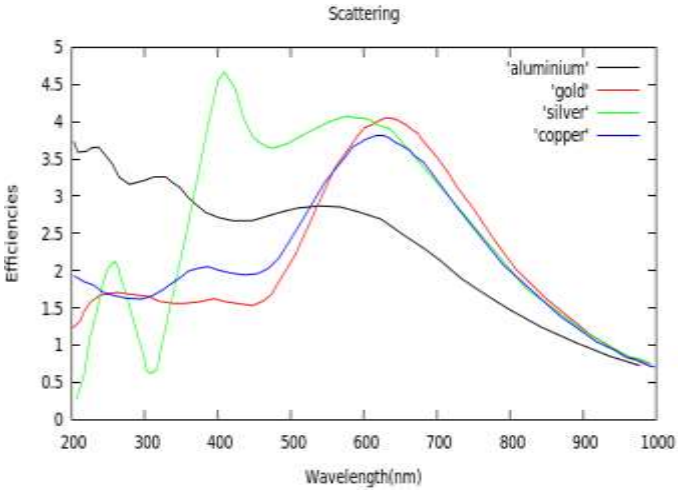

(f)

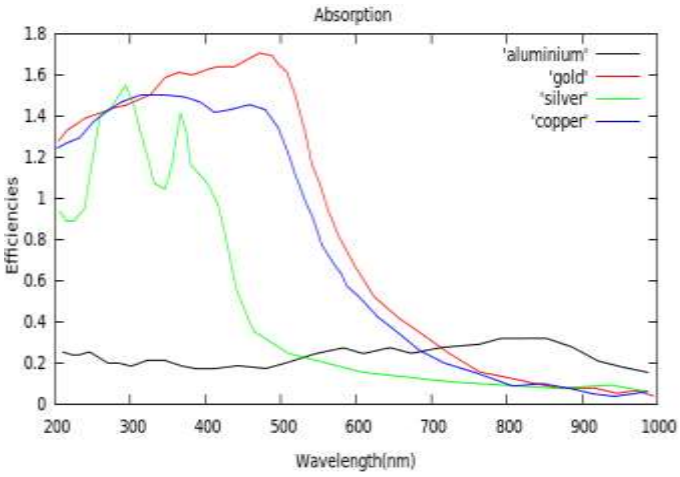

(g)

Fig. 3. Localised field distribution for (a) Silver, (b) Gold, (c) Aluminium, (d) Copper and (e) E_field variations with the incident illumination. (f) Mie scattering efficiency with (g) NP absorption efficiency.

In the shorter-wavelength region, plasmonic effect dominated by metallic absorption can be reduced by usage of Al NPs for stronger overall photocurrent. In a plasmonic analysis with the NPs, an interference between the incident light and NP scattered light termed as Fano effect is observed below the resonance frequency creating an insulation for radiations to enter the device. In case of Al, with the plasmon resonance in UV region where the solar irradiance is negligible, associated parasitic absorption is less with enhanced device performance[20]. The enhanced transmission is observed over the entire solar spectrum with Al due to its much smaller Fano reduction in the shorter wavelengths[21]. Even with good performance in the UV and blue region, it has not been widely used in plasmonics due to its higher oxidation rate.

3.1.4. Cu (Copper)

The highly abundant and less expensive Cu provides an alternative NP option for the plasmonic absorption in thin film solar cells. In the considered structure with Cu NPs deposited at the front surface, the plasmon resonance is observed with an incident wavelength of 465nm within the visible wavelength region as shown in Fig. 3(d). Cu as NP is chemically unstable and possesses absorption related losses which need to be overcoated to avoid getting it oxidized for obtaining higher power conversion efficiency. In the observed results, drastic improvement in power conversion efficiencies is observed with Cu because of low resistivity and strong interactions for the visible range of incident light wave making it a promising NP option for the plasmonic thin-film solar cell for our future needs. The reduced reflection of light at the shorter wavelengths indicates that with Cu NPs substantial loss is observed due to absorption of a large portion of the visible range incident radiations. The encapsulation of the Cu NPs in ITO layer will eliminate the oxidizing effects, creating an ideal environment for plasmonic resonance and with ease of manufacturing, it can be a big contender for future low-cost thin film solar cells.

The generated localised near-field plots for structures with Ag, Au, Al and Cr NPs shown in Fig.3 are used for comparison of electromagnetic interactions with the structures for obtaining the relative dependency of the electrical enhancement on the NP based on its permittivity values. The analysis covered a wide wavelength range from 200nm to 1000nm for properly identifying the incident wavelength at which corresponding NPs display surface plasmon resonance. It is observed that in short-wavelength region Al with negative ε' presents an ideal case with lower refractive index (*n*) and higher reflectivity (*k*) value satisfying the requirement for photovoltaics and the near to zero value of ε" for Ag, Au and Cu results in performance degradation due to the falling *k* value in the region of strong metallic absorption. It's known that with more negative ε' and higher positive ε" values, the higher will be *n* value. In a long-wavelength region, Al possesses larger *n* values when compared to Au, Ag and Cu resulting in the reduction of conversion efficiency with relatively higher metallic absorption. The obtained numerical results demonstrate that the structures with Ag NPs have higher conversion efficiency followed by Cu, Au and Al. The similar near-field intensity properties of Cu and Au will generate indistinguishable scattering of incident light with almost same intensity. Based on the simulated results it's observed that with the red-shift of the extinction peak for Al, Au, Ag and Cu NP's, the radiative efficiency doesn't decrease, making them potential

candidates for plasmonics in thin film solar cells. The optical properties of Ag, Au and Cu are very similar at higher wavelengths with slightly enhanced transmitted power compared to Al NPs. At the lower wavelengths of the visible region, Ag is preferred choice for its enhanced optical properties associated with interband transitions. The uncommon optical properties of Al with broader and weaker resonances in the visible region are excited in the UV region with higher device absorption near infra-red (IR) due to a weak interband region between valence and conduction band. Out of the considered NP's lowest losses is observed with Ag, followed by Au, Cu and Al.

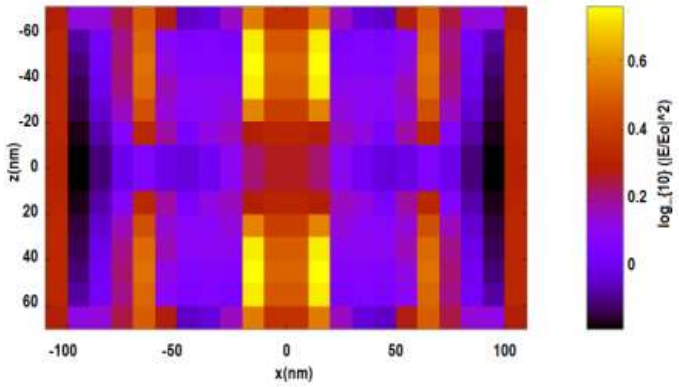

(a) Platinum @474nm

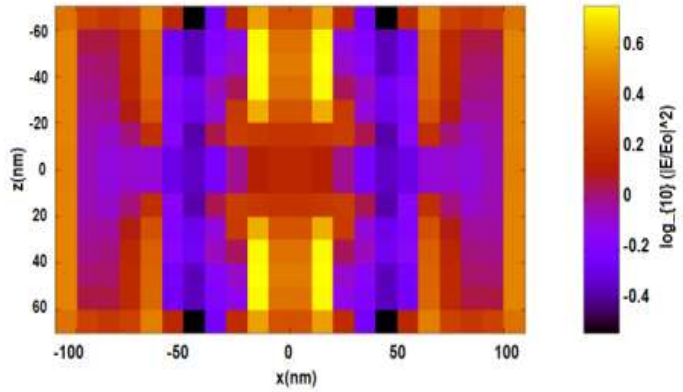

(b) Palladium @650nm

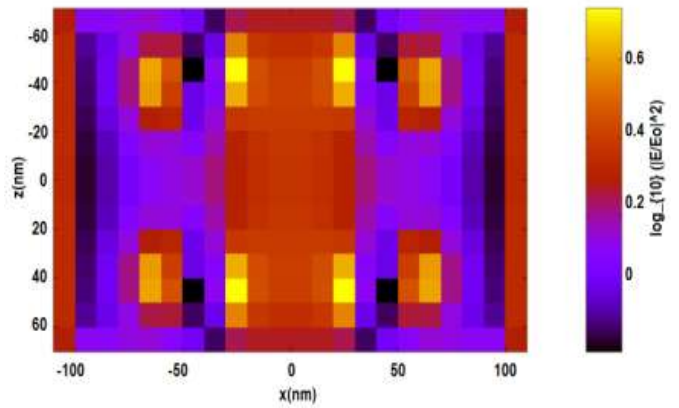

(c) Titanium @474nm

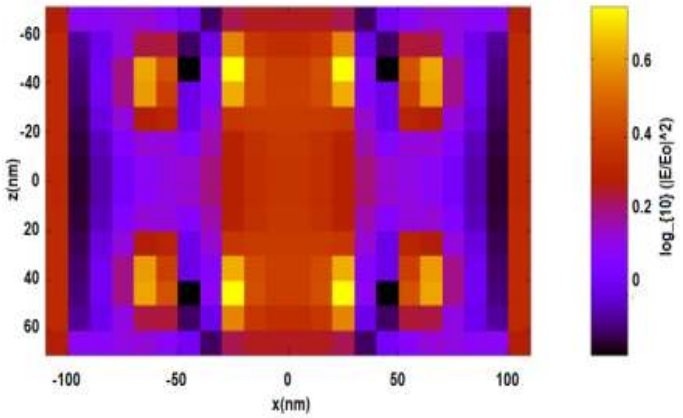

(d) Tungsten @474nm

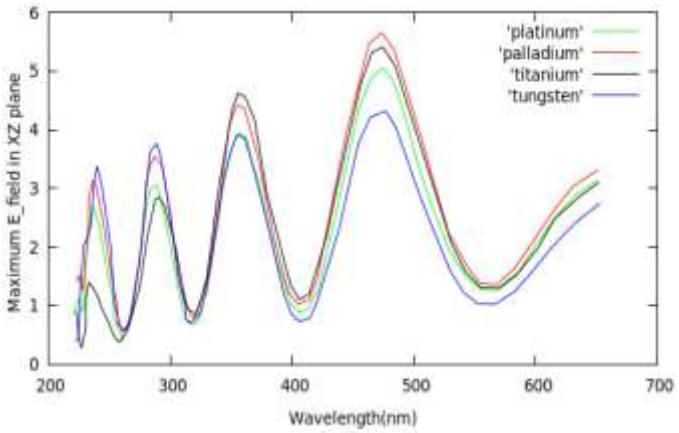

(e)

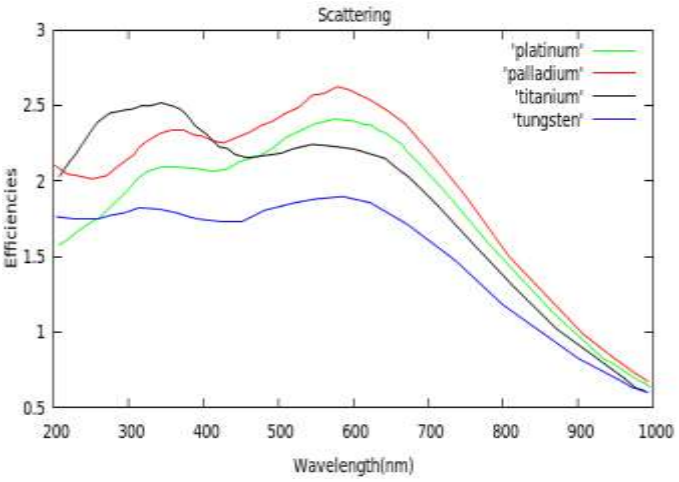

(f)

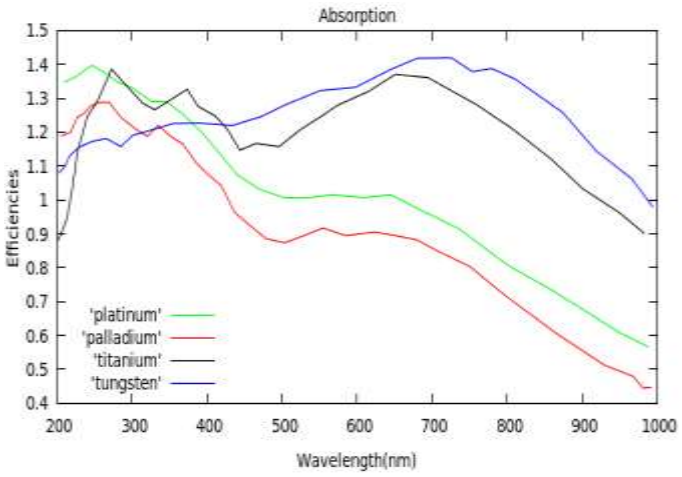

(g)

Fig. 4. Localised field distribution for (a) Platinum, (b) Palladium, (c) Titanium, (d) Tungsten, and (e) E_field variations with the incident illumination. (f) Mie scattering efficiency with (g) NP absorption efficiency.

3.2. Structures with Pt, Pd, Ti and W NPs

The computed electric field distributions for the Pt, Pd, W and Ti structures at Mie scattering resonances for the scattering and device absorption maxima are as shown in Fig.4. These materials with higher melting temperatures have superior performance compared to other noble metals. The catalytically much active Pt has distinct and well-defined absorption peaks in the visible region with the generated electric field not as scattered as Cu or Au, making it a poor reflector of the incident radiations. Compared to Ag, Pt and Pd NPs exhibit broader localized surface plasmon with a higher sensitivity. Unlike the widely studied Au and Ag nanostructures, which have distinct and well-defined SPR absorption peaks, these NPs exhibit broad extinction from the ultraviolet to short wavelength of visible light, without observable peaks. The highly resistive W has much higher damping coefficient than Au restricting the resonance at around 474nm in the blue region of the spectrum. Pd NPs reduce the initial reflection loss in the complete wavelength range noticeably below 500nm [22]. From the obtained results it's observed that structures with Pd NPs upon light being incident, generate a higher localised field and with higher scattering to absorption ratio possess higher conversion efficiency followed by Pt, Ti & W and in common have comparatively higher losses in the mid-IR region. With the resonance wavelength shift from 650nm to 474nm, blue-shift resonance is observed for Pt, Ti and W compared to Pd as shown in Fig.4 (a-d). The observed localised electric field variations as captured in Fig. 4(e) summarizes that the pattern variation for the field generation is same with magnitude values in the order of W, Pt, Ti and Pd where Pd has higher values, denoting higher e-h pair generation for the enhanced spread of the photon absorption within the device.

The calculated efficiencies based on the Mie scattering principle are captured in Fig. 4(f-g) for the varying incident wavelength. In the UV region, the dominant NP absorption over the scattering cross-sections makes the considered NPs as non-feasible options. With the increased wavelength till the yellow region of the visible spectrum, the scattering dominates the NP absorption resulting in enhanced device absorption and with more shift towards the red region, a sharp reduction in scattering and NP absorption efficiency is observed. The common trend of efficiency variation is seen with Pt, Pd and Ti reducing the reflection losses with a noticeable effect in the range of 400nm-650nm with the comparatively lesser scattering to absorption ratio compared to Ag or Au. For the case of W, the scattering to absorption ratio is affected by the dominant absorption over the scattering cross-section making it not a good choice option for plasmonic enhancement in thin film solar cells.

3.3. Structures with Br, Cr and Ni NPs

In this section, thin film structural analysis is carried out with Br, Cr and Ni as NPs on the front surface to explore the multiple options for an intense interaction with UV, visible and IR incident photons for the excitation of LSP. The observed localised field distribution at the interface of NPs and the dielectric medium upon the incident light illumination is as shown in Fig.5 (a-c) and the field variation with the incident wavelength variations pertaining to the selected NP is plotted in Fig. 5(d).

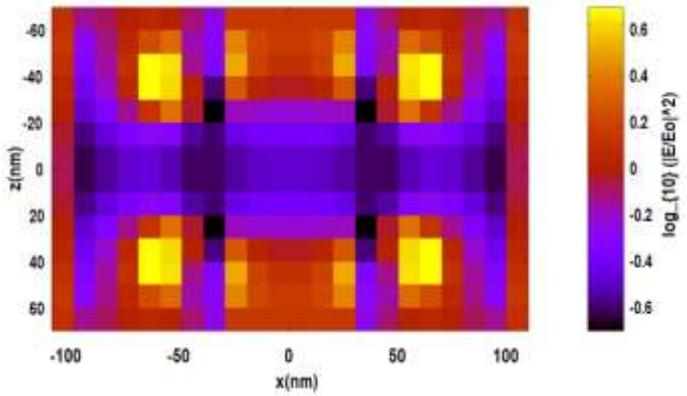

(a) Beryllium @247nm

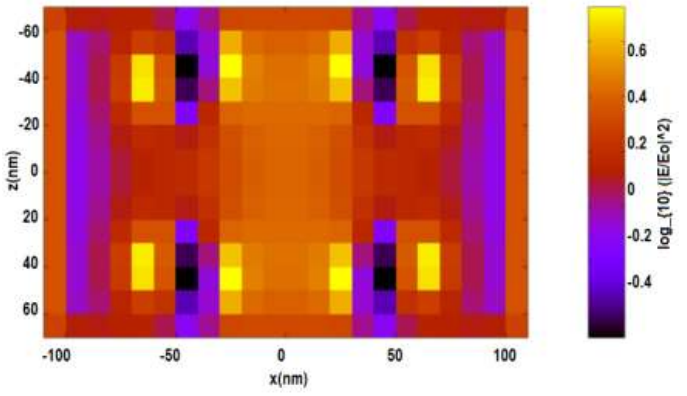

(b) Chromium @474nm

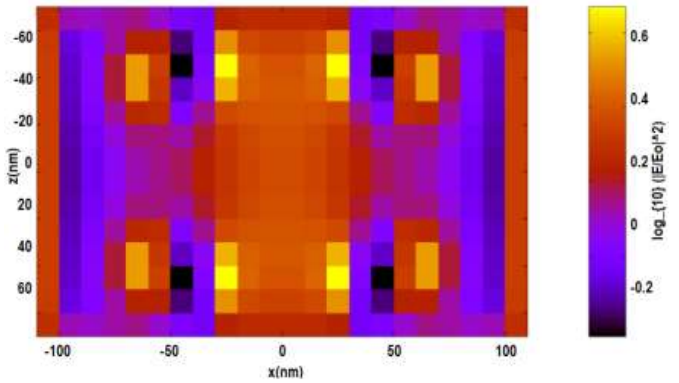

(c) Nickel @474nm

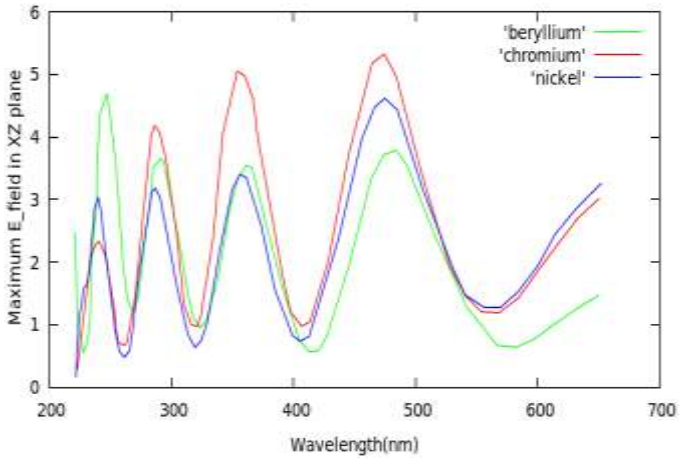

(d)

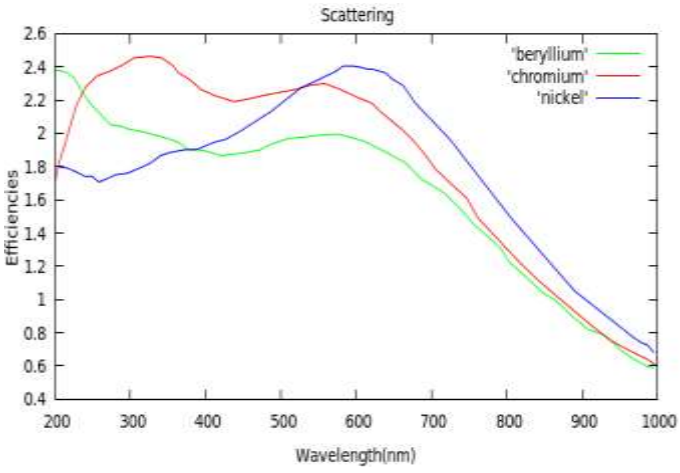

(e)

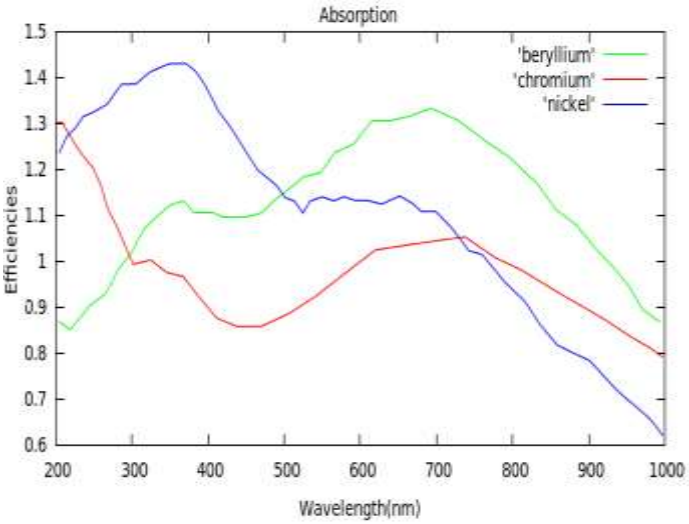

(f)

Fig. 5. Localised field distribution for (a) Beryllium, (b) Chromium, (c) Nickel and (d) E_field variations with the incident illumination. (e) Mie scattering efficiency with (f) NP absorption efficiency.

In the developed model with the considered NPs, obtained scattering and absorption efficiencies based on the Mie scattering principle are presented in Fig.5 (e-f). The soft and brittle Br can also become one of the best NP option as it possesses strong metallic property. A huge resemblance is observed between generated localised field distributions for Br and Al with observed resonance at around 247nm. The more blue shifted resonance has very less generated field spectra values in Br compared to Al in UV region. The heavy and highly toxic Cr is highly oxidisable. The observed resonance is weaker in Ni compared to Au owing to relatively higher ε" values. The widespread spectrum is observed with Cr and Ni NPs with the resonance at around 474nm similar to comparatively lesser spread Pt. The field value variations of Ni follow Cr with lesser value as shown in Fig. 5(d). As observed with Ni and Cr, near to the ultraviolet region scattering to absorption ratio is dominated by the parasitic absorption whereas in Br it's a dominant scattering over the absorption. For the considered NPs in the wavelength range of around 400nm-600nm, comparatively higher scattering over absorption is observed followed by the dominant absorption over the falling scattering in the near IR region making Br, Cr and Ni better suited for higher scattering in the mid-IR region of the visible spectrum. The maximum field enhancements observed with that of the commonly used metals Au, Cu and Ag are 20% lower than the ideal metals due to the higher attenuation caused by the excitation of surface plasmons in the visible range of the spectrum.

3.4. Structures with Nitride NPs

The dielectric nitrides possessing chemical stability at higher temperatures with metallic behaviour are known for their refractory properties. The considered nitrides have plasmonic properties in the visible and near-infrared range as they have zero cross over wavelength in the region. In the

noble metals, higher ε" with large plasma frequency translates to higher losses whereas in nitride NPs with relatively lower carrier concentration parasitic losses are reduced [17]. For nitrides to achieve negative permittivity values, the free carrier concentration is typically increased through impurity doping, higher the carrier concentration they start behaving like metals providing a potential alternative for plasmonic applications. The structures with the metal nitrides as NPs generate similar enhancement compared to the noble metals with very less dissipative losses at the visible wavelengths and observed potential transparency suppresses design-related problems in the thin film solar cells. The absence of Fano effect in the low-dispersive nitrides with better trapping effects [23] makes them the best available option for plasmonics in thin film a-Si:H solar cells over the highly absorbing metals. In the visible wavelength range with higher negative ε' value, dielectric nitride NPs [24] exhibit enhancement in field distribution providing higher scattering, increasing the incident light being trapped. The choice of a dielectric as NP is a compromise between high dielectric permittivity and low dissipation level.

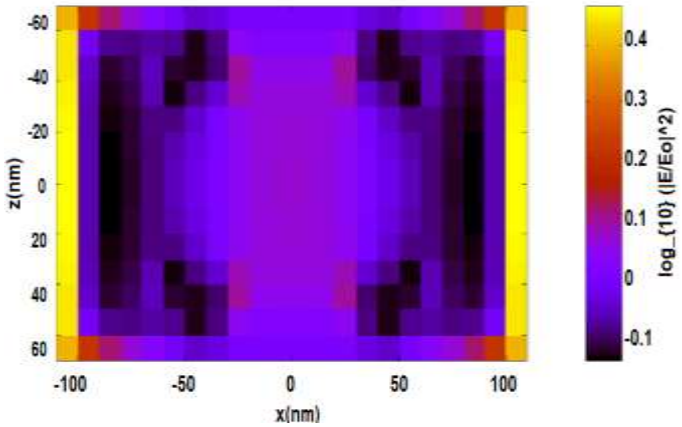

(a) ZrN @650nm

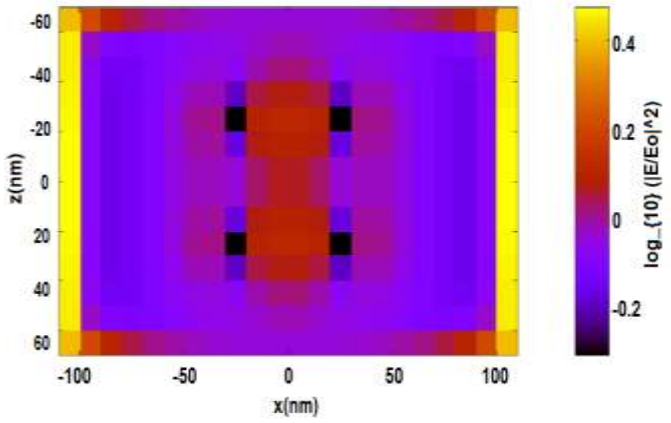

(b) TaN @650nm

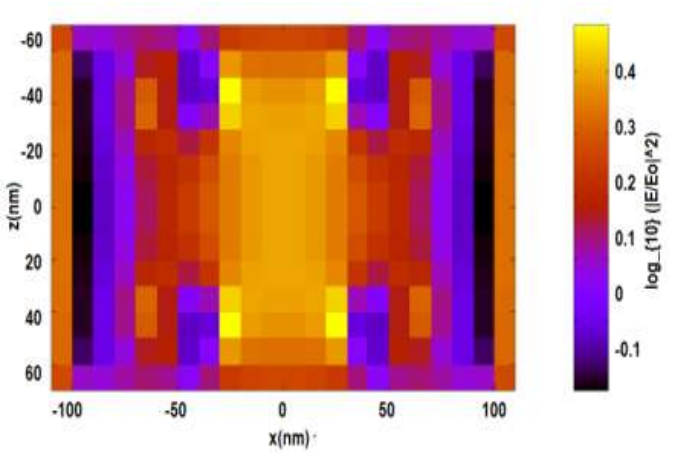

(c) HfN @474nm

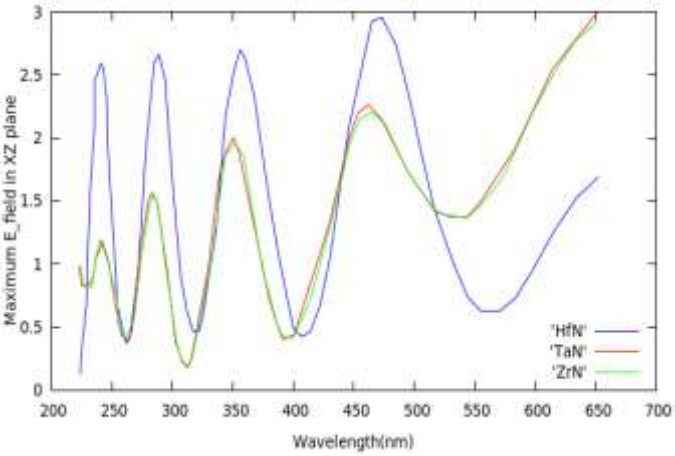

(d)

Fig. 6. Localised field distribution for (a) ZrN, (b) TaN, (c) HfN, and (d) E_field variations with the incident illumination.

The observed resonance for Tantalum Nitride (TaN) and Zirconium Nitride (ZrN) are similar to Au in magnitude and wavelength as shown in Fig.6 with higher temperature sustainability. In case of HfN, the resonance wavelength is similar to Ag with a comparatively lesser magnitude of the generated field. The ε' transition in ZrN and TaN within the visible region over the constant ε' values for HfN, results in the red-shift of the resonance wavelength from 474nm to 650nm. The reduced nanofabrication problems in nitrides compared to Au and Ag makes them viable alternative plasmonic material [25]. From the simulated results, it's observed that nitrides are poor near-field enhancers compared to noble metals at their respective resonance wavelengths, with the observed fields for ZrN and TaN NPs are 60% less than that of Au NPs. The promising capabilities of nitrides over the noble metals can be the best future possible plasmonic option in sync with standard semiconductor manufacturing technology.

The optical scattering and parasitic absorption of front NPs are closely related to the response of each NP and the surrounding environment. With the developed model based on the underlying concepts of device physics and the theoretical correlation between the refractive index *(N= n+ik)* and the dielectric value of the NP material are explored

to understand the light trapping in thin photoactive layers of a-Si:H solar cell. Our results showed that the desired particle refractive index should have a small real part (*n*) and a large imaginary part (*k*), with higher *n* leading to degraded forward scattering into the device and with the slight deviation of *k* it decreases rapidly. For the lower *n* and higher *k*, the dielectric value of the NP material ε' should have higher negative value whereas ε" should have more positive value as almost no NP absorption happens and simultaneously able to manipulate light effectively into the device. The scattering cross-section of a plasmonic NP can be as high as 10 times larger than the geometrical cross-sections resulting in 100% scattering within the device with 10% surface coverage of NPs. The scattering cross sections are spectral dependent with spectral position variation through modification of the NP choice and surrounding material. All the results show that variety of metal types provides different advantages over some shortcomings and the choice of type of NP for light scattering to be made on the basis of wavelength range target for the structure.

4. Conclusion

In this paper, a variety of highly conducting metals and low-cost metal nitrides are compared for surface plasmonic effects in terms of achieving higher device scattering for trapping the incident light within the device. The obtained results can be summarized as: observed resonance for structures with aluminium and beryllium NPs is in the UV region, followed by the resonance shift to 450-600nm range with silver, copper, chromium, nickel, platinum, titanium, tungsten NPs where they can absorb around 90% of the incident power with more red-shift in resonance observed in gold, palladium NPs at around 650nm, enhancing the efficiency by coupling and scattering the incoming light into the device to increase the effective optical path length. With the considered metal NPs for confining light into the active layer at the cost of associated parasitic losses can be replaced by low-cost nitrides for avoiding Fano effects and associated heat losses. The observed resonances of TaN, ZrN are similar to gold and HfN are with silver can be the best option for absorbing the red-spectrum for the already observed blue light by active a-Si:H layers with needed enhancement in localised field generation. The comparative analysis enables with the proper choice of suitable NP for higher absorption range and efficiency enhancement determined by low dissipative and low-dispersive material over highly absorbing metals for thin film solar cells.

References

[1] Al-Khazzar, “Behavior of Four Solar PV Modules with Temperature Variation”, International Journal of Renewable Energy Research, Vol 6, No 3, pp 1091-1099, 2016.

[2] H. Aguas, S. K Ram, A. Araujo, D. Gaspar, A. Vicente, S.A Filonovich, E. Fortunato, R. Martins, I. Ferreira, “Silicon thin film solar cells on commercial tiles”, Energy Environ. Sci., Vol 4, No 11, 4620–4632, 2011.

[3] S. A. Filonovich, P. Alpuim, L. Rebouta, J. E. Bourée, Y. M. Soro, “Hydrogenated amorphous and nanocrystalline silicon solar cells deposited by HWCVD and RF-PECVD on plastic substrates at 150 °C”, Journal of Non-Crystalline Solids, Vol 354, pp 2376–2380, 2008.

[4] Ibrahim, A. A. El-Amin, “Temperature Effect on the Performance of N-type µc -Si Film Grown by Linear Facing Target Sputtering for Thin Film Silicon Photovoltaic Devices”, International Journal of Renewable Energy Research, Vol 2, No 1, pp 160-165, 2012.

[5] K. Patel, P. K. Tyagi, “Technological Advances in a-Si:H/c-Si Heterojunction Solar Cells”, International Journal of Renewable Energy Research, Vol 4, No 2, pp 528-538, 2014.

[6] H. A. Atwater, A. Polman, “Plasmonics for improved photovoltaic devices”, Nature Materials, Vol 9, pp 205-213, 2010.

[7] H. Raether, “Surface polaritons on smooth and rough surfaces and on gratings”, Springer-Verlag, Berlin, 1988.

[8] U. Kreibig, M. Vollmer, “Optical Properties of Metal Clusters”, Springer, Vol 25, 1995.

[9] F. Bohren, D. R. Huffman, “Absorption and Scattering of Light by Small Particles”, Weinheim: Wiley, 2004.

[10] K. R. Catchpole, A. Polman, "Plasmonic solar cells", Optics Express, Vol 16, pp 21793-21800, 2008.

[11] Chetan Radder, B S Satyanarayana, “FDTD based plasmonic light trapping analysis in thin film hydrogenated amorphous silicon solar cells”, International Journal of Renewable Energy Research, Vol 8, No 1, pp 514-522, 2018.

[12] A F Oskooi, D Roundy, M Ibanescu, P Bermel, J D Joannopoulos, S G Johnson, “MEEP: A flexible free software package for electromagnetic simulations by the FDTD method”, Computer Physics Communications, Vol 181, No 3, pp 687-702, 2010.

[13] P R West, S Ishii, G V Naik, N K Emani, V M Shalaev, A Boltasseva, “Searching for better plasmonic materials”, Laser Photonics, Vol 4, No 6, pp 795–808, 2010.

[14] A Vora, J Gwamuri, J M Pearce, P L Bergstrom, D Ö. Guney, “Multi resonant silver nano-disk patterned thin film hydrogenated amorphous silicon solar cells for Staebler-Wronski effect compensation”, Journal of Applied Physics, Vol 116, No 9, 2014.

[15] Y. Premkumar Singh, Amit Jain, Avinashi Kapoor, “Localized Surface Plasmons enhanced light transmission into c-Silicon Solar Cells”, Journal of Solar Energy, Vol 2013, Article ID 584283, 6 pages, 2013.

[16] Edward Palik, “Handbook of optical constants of solids”, Academic Press, Elsevier Science, pp 350-356, 1985.

[17] G V Naik, J Kim, A Boltasseva, “Oxides and nitrides as alternative plasmonic materials in the optical range”, Optical Materials Express, Vol 1, No 6, pp 1090-1099, 2011.

[18] M. J. Mendes, S. Morawiec, T. Mateus, A. Lyubchyk , H. Aguas, I. Ferreira , E. Fortunato, R. Martins, F. Priolo, I. Crupi, “Broadband light trapping in thin film

solar cells with self-organized plasmonic nanocolloids", Nanotechnology, Vol 26, No 13, pp 2015.

[19] N. C. Lindquist, P. Nagpal, K M McPeak, D. J. Norris, Sang-Hyun Oh, "Engineering metallic nanostructures for plasmonics and nanophotonics", Reports on Progress in Physics, Vol 75, No 3, 2012.

[20] K. Singh, A. Jain, A. Kapoor, "Enhancement in light coupling into silicon solar cells using low cost and earth abundant aluminium nanoparticles", International Journal of Engineering and Applied Sciences, Vol 1, No 3, pp 86-90, 2013.

[21] F. Villesen, C. Uhrenfeldt, B. Johansen, J. L. Hansen, H. U. Ulriksen, A. N. Larsen, "Aluminium nanoparticles for plasmon-improved coupling of light into silicon," Nanotechnology, Vol 23, No 8, 2012.

[22] M. Atyaoui, A. Atyaoui, M. Khalifa, J. Elyagoubi, W. Dimassi, H. Ezzaouia, "Enhancement in photovoltaic properties of silicon solar cells by surface plasmon effect of palladium nanoparticles", Superlattices and Microstructures, Vol 92, pp 217-223, 2016.

[23] P. Vasudev, J. A. Schuller, M. L. Brongersma, "Nanophotonic light trapping with patterned transparent conductive oxides," Optics Express, Vol 20, No S3, pp A385–A394, 2012.

[24] Yu. A. Akimov, W. S. Koh, S. Y. Sian, S. Ren, "Nanoparticle-enhanced thin film solar cells: Metallic or dielectric nanoparticles?", Applied Physics Letters, Vol 96, No 7, 2010.

[25] G V Naik, J L. Schroeder, Xingjie Ni, A V. Kildishev, T D. Sands, A Boltasseva, "Titanium nitride as a plasmonic material for visible and near-infrared wavelengths", Optical Materials Express, Vol 2, No 4, pp 478-479, 2012.